Ca^{2+}-binding activity of a COOH-terminal fragment of the *Drosophila* BK channel involved in Ca^{2+}-dependent activation

Shumin Bian*, Isabelle Favre*†, and Edward Moczydlowski*‡§

Departments of *Pharmacology and ‡Cellular and Molecular Physiology, Yale University School of Medicine, 333 Cedar Street, New Haven, CT 06520-8066

Communicated by Ramon Latorre, Center for Scientific Studies of Santiago, Valdivia, Chile, February 13, 2001 (received for review November 28, 2000)

Mutational and biophysical analysis suggests that an intracellular COOH-terminal domain of the large conductance Ca^{2+}-activated K^+ channel (BK channel) contains Ca^{2+}-binding site(s) that are allosterically coupled to channel opening. However the structural basis of Ca^{2+} binding to BK channels is unknown. To pursue this question, we overexpressed the COOH-terminal 280 residues of the *Drosophila slowpoke* BK channel (Dslo-C280) as a FLAG- and His_6-tagged protein in *Escherichia coli*. We purified Dslo-C280 in soluble form and used a $^{45}Ca^{2+}$-overlay protein blot assay to detect Ca^{2+} binding. Dslo-C280 exhibits specific binding of $^{45}Ca^{2+}$ in comparison with various control proteins and known EF-hand Ca^{2+}-binding proteins. A mutation (D5N5) of Dslo-C280, in which five consecutive Asp residues of the ''Ca-bowl'' motif are changed to Asn, reduces $^{45}Ca^{2+}$-binding activity by 56%. By electrophysiological assay, the corresponding D5N5 mutant of the *Drosophila* BK channel expressed in HEK293 cells exhibits lower Ca^{2+} sensitivity for activation and a shift of ≈+80 mV in the midpoint voltage for activation. This effect is associated with a decrease in the Hill coefficient (N) for activation by Ca^{2+} and a reduction in apparent Ca^{2+} affinity, suggesting the loss of one Ca^{2+}-binding site per monomer. These results demonstrate a functional correlation between Ca^{2+} binding to a specific region of the BK protein and Ca^{2+}-dependent activation, thus providing a biochemical approach to study this process.

Large conductance Ca^{2+}-activated K^+ channels (BK channels) are synergistically activated by membrane depolarization and intracellular Ca^{2+} (1). They are widely distributed in neurons and smooth muscle, where they respectively function in regulating the release of neurotransmitter and cell contractility. Although BK channels can be activated by high positive voltage (>+100 mV) in the virtual absence of Ca^{2+} (<1 nM) (2, 3), an increase in local Ca^{2+} concentration shifts the voltage activation threshold toward the physiological voltage range. The BK channel protein is structurally related to tetrameric voltage-gated K^+ channels by homology within an S1–S6 region that contains the pore-forming domain, S5-P-S6, and an S4 voltage-sensing element (4); however, it also includes an additional NH_2-terminal transmembrane span, S0 (5), and a unique COOH-terminal sequence of ≈850 residues (see Fig. 1). Sequence analysis identified four hydrophobic segments in the C-terminal region, S7–S10, as potential transmembrane spans (4), but recent evidence shows that S9 and S10 are contained within cytoplasmic domain(s) (5).

Current models of BK channel gating propose that consecutive binding of one Ca^{2+} ion per monomer of a homotetrameric complex promotes channel opening in a cooperative reaction that is allosterically coupled to a cooperative voltage-dependent gating mechanism (6, 7). This complex mechanism shares basic features in common with the Monod-Wyman-Changeux model for allosteric activation of a tetrameric enzyme (8). Structure-function analysis indicates that the BK channel protein can be dissected into conserved ''Core'' and ''Tail'' domains that are separated by a nonconserved linker region (9). The Core corresponds to the NH_2-terminal part of the protein containing S0–S6 plus a portion of the COOH terminus, whereas the ≈400 residue sequence following the linker comprises the Tail (Fig. 1). Experiments with chimeric Core-Tail constructs by using Slo1 genes of different species suggest that the Ca^{2+}-sensing function of the channel is associated with the Tail domain (9). More recent studies making use of the Ca^{2+}-insensitive Slo3 K^+ channel gene verified that specific regions of protein sequence within the Tail confer the property of Ca^{2+}-dependent gating (10). Complementary mutational studies identified an Asp-rich sequence motif in the Tail domain (Fig. 1), called the ''Calcium Bowl'' (Ca-bowl), as a possible site(s) of Ca^{2+} binding (11).

Despite this progress, the structural basis of Ca^{2+} binding to the BK channel protein and the mechanism by which Ca^{2+} binding is coupled to channel opening are poorly understood. To pursue this problem, we adopted a biochemical approach to assay and localize Ca^{2+} binding sites. This assay employs a $^{45}Ca^{2+}$-overlay technique that has been used to identify other Ca^{2+}-binding proteins: e.g., proteins that contain EF-hand motifs such as calmodulin (12, 13). We overexpressed in *Escherichia coli* the COOH-terminal 280 residues of the *Drosophila* BK channel (Dslo-C280) containing the Ca-bowl region. This protein was purified and found to exhibit $^{45}Ca^{2+}$ binding activity comparable to calmodulin. The functional significance of such activity was examined by mutating five consecutive Asp residues in the Ca-bowl to Asn and comparing the $^{45}Ca^{2+}$-signal with Ca^{2+}-activation of the channel by electrophysiological analysis. The results demonstrate a direct correlation between Ca^{2+} binding and Ca^{2+} sensitivity for channel activation. This soluble Ca^{2+}-binding domain thus represents a promising candidate for structural analysis of ligand binding central to the mechanism of BK channel gating.

Materials and Methods

Construction of the Ca-Bowl Mutant D5N5 and Expression of Dslo. A pRc/cytomegalovirus (CMV) vector (Invitrogen) containing the coding sequence of an alternatively spliced variant (A1C2E1G3I0) of the *Drosophila* BK channel (Dslo) described by Adelman *et al.* (14) was generously supplied by Dr. Irwin Levitan (University of Pennsylvania). In sequencing this clone, we noted the presence of one conservative mutation, D964E (see Fig. 1*C*) that varied from the reported wild-type sequence (14). Silent mutations were used to introduce two unique restriction sites flanking the Ca-bowl motif (11). These sites were used to

Abbreviations: BK channel, large conductance Ca^{2+}-activated K^+ channel; Dslo, *Drosophila* BK channel; Dslo-C280, COOH-terminal 280 residues of Dslo; IPTG, isopropyl β-D-thiogalactoside; NTA, nitrilotriacetic acid; SEC, size exclusion chromatography.

†Present address: Department of Physiology, Centre Medical Universitaire (CMU), 1, Rue Michel Servet, 1211 Geneva 4, Switzerland.

§To whom reprint requests should be addressed at: Department of Pharmacology, Yale University School of Medicine, P.O. Box 208066, New Haven, CT 06520-8066. E-mail: edward.moczydlowski@yale.edu.

The publication costs of this article were defrayed in part by page charge payment. This article must therefore be hereby marked "*advertisement*" in accordance with 18 U.S.C. §1734 solely to indicate this fact.

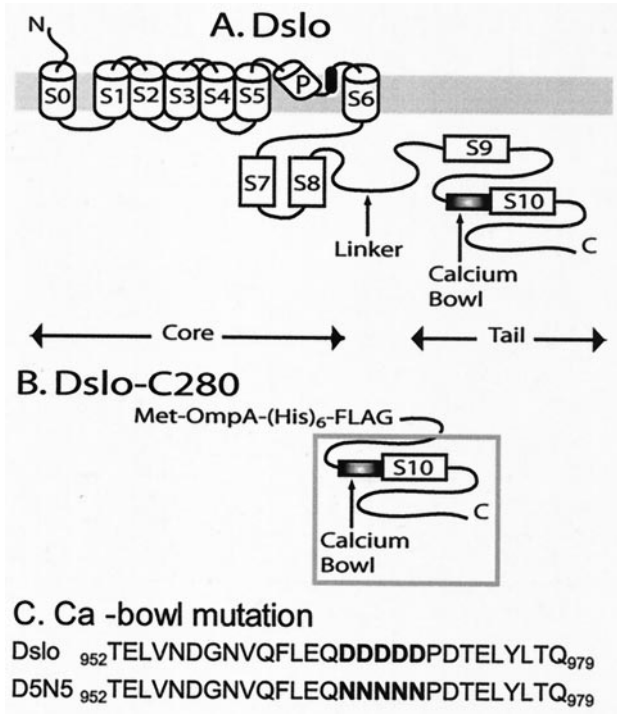

Fig. 1. Schematic overview of *Drosophila* BK channel and expressed fragment. (*A*) Topology diagram of Dslo α subunit showing the location of Core and Tail domains. (*B*) Construction of Dslo-C280 protein (and D5N5 mutant) expressed in *E. coli*. (*C*) Sequence of Ca-bowl motif (Dslo residues T952-Q979) of Dslo-C280 and D5N5 mutant.

generate the mutant Dslo channel, D5N5, in which five consecutive Asp residues in the Ca-bowl region D966-D970 were changed to Asn by PCR mutagenesis (15). All constructions were verified by DNA sequencing. The restriction fragment containing the D5N5 mutant was subcloned into the pcDNA3.1 mammalian cell expression vector (Invitrogen) and used to transfect HEK293 cells with the Effectene Kit from Qiagen (Chatsworth, CA). Methods for producing a stably transfected HEK293 cell line expressing the parent Dslo clone were reported previously (16).

Construction and Bacterial Expression of COOH-Terminal Protein Fragments Dslo-C280 and C280-D5N5. A restriction fragment coding for the last 280 aa of Dslo was inserted in frame into the bacterial expression vectors pFLAG-ATS and pH_6FLAG-ATS. pFLAG-ATS is a commercial (Sigma) vector for FLAG-tagged expression of foreign proteins in *E. coli*. This vector adds an NH_2-terminal OmpA signal sequence, followed by an eight-residue FLAG epitope sequence (DYKDDDDK). The related pH_6FLAG-ATS vector was constructed by adding a hexahistidine (His_6) coding sequence to pFLAG-ATS inserted after the OmpA signal sequence and directly before the FLAG sequence, as illustrated in Fig. 1. For protein production, vector-transformed *E. coli* strain BL21 (Stratagene) was grown in LB media at 22°C, and induced by adding 0.2 mM isopropyl β-D-thiogalactoside (IPTG).

Fractionation of Dslo-C280 and C280-D5N5. Analytical fractionation of FLAG-tagged Dslo fusion proteins followed protocols in the Sigma FLAG *E. coli* Expression System Manual. A sucrose-based osmotic shock procedure was used for isolation of periplasmic proteins. Whole cells were lysed with lysozyme by using extraction buffers containing DNAaseI, and ovomucoid or aprotinin protease inhibitors. The whole cell soluble fraction was collected after centrifugation at 20,000 $\times$ *g* for 0.5 h. The pellet, containing whole cell insoluble protein, was washed thoroughly in 50 mM Tris·HCl (pH 8.0), 500 mM NaCl, 0.2% Tween 20, 10 mM EDTA, and finally in 50 mM Tris·HCl (pH 8.0) and 150 mM NaCl. Washed inclusion body protein was solubilized by denaturation in 6 M guanidine-HCl for 12 h at 4°C with shaking. Refolding was achieved by dialysis in 50 mM Tris·HCl (pH 8.0), 150 mM NaCl, 10% glycerol, and stepwise reduction of guanidine HCl (4 M to 0 M) and DTT (5 mM to 0 mM) over the course of 3 days at 4°C. Chemiluminescent detection of FLAG-tagged Dslo protein on immunoblots probed with M2 anti-FLAG antibodies (Sigma) was performed according to the supplier's (Pierce) protocol.

Purification of Dslo-C280 and C280-D5N5. Both FLAG-based and His_6-based affinity methods were used in purifying soluble and refolded Dslo protein. M2 anti-FLAG agarose was used according to the manufacturer's (Sigma) instructions. In the final step, the M2 column was eluted with 5 column volumes of 100 μg/ml FLAG peptide. The His_6-based method, applied to purifying Dslo protein from inclusion bodies, combines purification and renaturation in one step on a Ni^{2+}-nitrilotriacetic acid (NTA; Amersham Pharmacia) column at 4°C. The start buffer, composed of 5 mM imidazole, 40 mM Tris·HCl (pH 8.0), 6 M guanidine-HCl, 0.5 M NaCl, and 1 mM β-mercaptoethanol, was used for solubilizing inclusion bodies and loading the protein sample onto a 5-ml Ni^{2+}-NTA column. The column was then eluted with 20 bed volumes of wash buffer (15 mM imidazole/20 mM Tris·HCl, pH 8.0/6 M guanidine-HCl/0.5 M NaCl/1 mM β-mercaptoethanol) to remove extraneous protein. The refolding process was performed over 20 h with the application of a gradient starting from wash buffer (150 ml) mixed linearly with an equal volume of refolding buffer (15 mM imidazole/40 mM Tris·HCl, pH 6.8/0.5 M NaCl/1 mM β-mercaptoethanol). Refolded His_6-tagged protein was finally eluted from the Ni^{2+}-NTA column with 0.5 M imidazole, 0.5 M NaCl, 2 mM β-mercaptoethanol, adjusted to pH 8.0 with acetic acid. Either zwittergent 3–12 (2 mM) or dodecylmaltoside (5 mM) was added before protein concentration and storage to reduce aggregation. High performance size exclusion chromatography (SEC) used a TSK G3000SW column (7.5 $\times$ 600 mm; Tosoh Biosep). The isocratic elution buffer was 20 mM Hepes-NaOH (pH 7.2), 300 mM ammonium acetate, 10 mM CHAPS detergent, and 10 mM DTT.

$^{45}Ca^{2+}$ Overlay Assay. After SDS/PAGE, protein bands were electroblotted onto poly(vinylidene difluoride) membrane. The blot was extensively washed for 2 $\times$ 10 min and then 3 $\times$ 15 min by using 20 ml of wash buffer each time (10 mM imidazole-HCl, pH 6.7/70 mM KCl/0.5 mM $MgCl_2$). $^{45}Ca^{2+}$ overlay assay (14, 15) was performed by incubating the blot with 2 μM $^{45}CaCl_2$ (21 mCi/mg, NEN) in 20 ml wash buffer at 22°C for 1 h, followed by 3 $\times$ 2 min washes in deionized H_2O and 1 $\times$ 2 min in 50% ethanol. After the blot was air dried, it was exposed to Hyperfilm MP (Amersham Pharmacia) for 48 h. After developing the film, the poly(vinylidene difluoride) blot was stained for all proteins with Coomassie blue R250. Bands detected by $^{45}Ca^{2+}$- autoradiography and Coomassie blue were recorded on an IS-1000 digital imaging system (Alpha Innotech, San Leandro, CA). Relative peak areas of bands were measured by using densitometry software. For quantitative comparison, Dslo-C280 and C280-D5N5 protein was measured with the BCA protein assay (Pierce).

Patch Clamp Experiments. HEK293 cells were cultured at 37°C in DMEM media (GIBCO/BRL) supplemented with 10% FBS, 45 units/ml penicillin, and 45 mg/ml streptomycin. Cells stably transfected with the parent Dslo channel (16) were grown in the

presence of 0.9 mg/ml G418 (GIBCO/BRL). Gigaohm patch recordings in the inside-out mode were performed by using an EPC-9 amplifier and PULSE-PULSEFIT software (HEKA Electronics, Lambrecht/Pfalz, Germany). Firepolished micropipettes pulled from Corning 7052 capillary glass had a resistance of ≈8 MΩ in recording solution. The pipette solution (extracellular) was 100 mM K^+-gluconate, 2 mM KCl, 1 mM $MgCl_2$, 1 mM $CaCl_2$, 1.3 mM EGTA, 10 mM Hepes-KOH (pH 7.3). The bath solution (intracellular) was 103 mM K^+-gluconate, 5 mM KCl, 10 mM Hepes-KOH (pH 7.3). Bath solution was treated with Chelex 100 resin (Sigma) to reduce Ca^{2+} to trace levels, and solutions containing 10 to 1,000 μM Ca^{2+} were prepared by adding $CaCl_2$.

Results

Expression and Purification of Dslo-C280. Sequence coding for 280 COOH-terminal residues of Dslo, the *Drosophila slowpoke* gene product, was cloned into the pFLAG-ATS bacterial expression vector. As illustrated in Fig. 1*B*, this vector directs synthesis of a protein that has an NH_2-terminal OmpA secretory signal peptide (21 residues), followed by an optional $(His)_6$ tag, the FLAG epitope sequence (DYKDDDDK), eight residues (VKLLENSR) from the multiple cloning site, and 280 residues of DSlo. When vector-transformed *E. coli* BL21 cells were grown and fractionated, the Dslo-C280 protein was found in both soluble and insoluble fractions. Immunoblot detection by using M2 monoclonal antibody specific for the Flag-epitope verified that expression of a ≈34-kDa FLAG-tagged band was observed only when the cells were induced with IPTG (Fig. 2*A*, lane 1 vs. lanes 2–6). This FLAG-tagged protein was present in the pellet from lysed cells as well as in the high-speed supernatant (Fig. 2*A*, lanes 2 and 3), and was also present in soluble fractions of periplasmic protein released from osmotically shocked cells (Fig. 2*A*, lanes 5 and 6). These results indicate that *E. coli* secretes a certain amount of DSlo-C280 into the periplasm as a soluble protein, but that much of this protein is retained within the cell in the form of insoluble inclusion bodies, as typically observed for overexpression of many eukaryotic proteins in *E. coli*.

Dslo-C280 protein was purified both from the soluble bacterial extract and from inclusion protein first denatured in guanidine-HCl and refolded during dialysis. Figure 2*B* illustrates immunoaffinity purification by using an anti-Flag M2 column and specific elution with FLAG peptide. A FLAG-tagged band of the expected size (≈34 kDa) was observed for both types of samples, in addition to a few contaminant bands, for the originally soluble (Fig. 2*B*, lane 4) and refolded preparations (Fig. 2*B*, lane 5). In general, the inclusion protein fraction yielded a greater amount of pure DSlo-C280 (e.g., Fig. 2*B*, lane 5).

The purified FLAG-tagged Dslo-C280 protein is quite soluble; however, we found that concentrated samples tend to form a large aggregate (>200 kDa) as indicated by its appearance in the void volume when injected onto a high performance size exclusion column. By testing various detergents, we found that this aggregate could be disrupted into smaller complexes. Dslo-C280 protein pretreated with 20 mM Zwittergent C3–12 or 15 mM dodecylmaltoside was found to migrate on the SEC column as three distinct protein peaks (not shown) at elution volumes that nominally correspond to monomer (≈34 kDa), dimer (≈68 kDa), and a larger complex (≈140 kDa). SDS/PAGE analysis of Dslo-C280 taken from the dimer and monomer peaks of the SEC fractionation is illustrated in Fig. 2*C*, lanes 2 and 3, respectively. This experiment confirmed that Dslo-C280 can exist as a monomeric species in the presence of a mild detergent, but it also showed that this protein has a tendency to aggregate by forming dimers and higher oligomers.

A $(His)_6$ tag sequence was introduced before the FLAG tag sequence in another version of Dslo-C280. This protein and a corresponding $(His)_6$-FLAG-tagged Ca-bowl mutant (D5N5) were separately expressed in *E. coli* and purified by metal chelate affinity chromatography. This method allowed us to efficiently combine purification and refolding of the denatured inclusion body protein into one step (17). Purification of the $(His)_6$-tagged protein by elution of the Ni^{2+}-NTA column with imidazole is shown by SDS/PAGE analysis in Fig. 2*C*. Together, studies of Fig. 2 demonstrate that a soluble protein corresponding to the C-terminal 280 residues of Dslo can be synthesized in *E. coli* and purified in soluble form after refolding from inclusion protein.

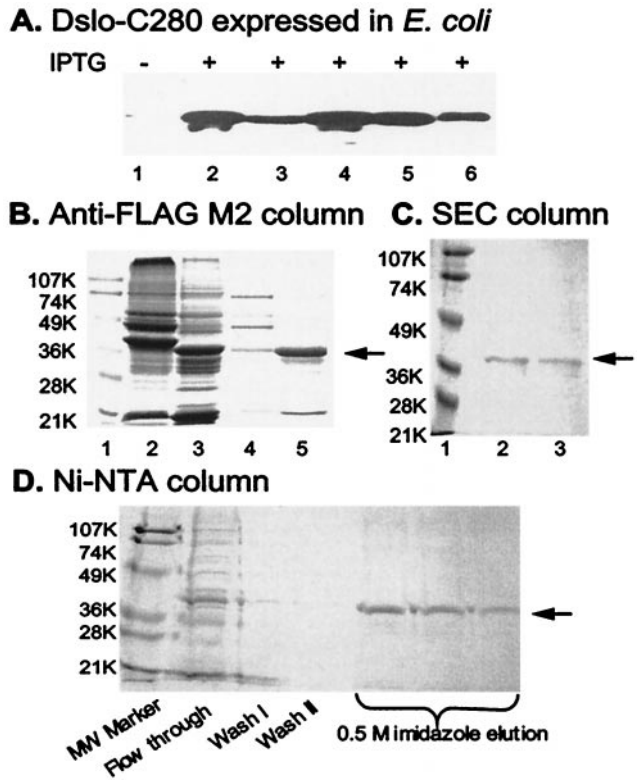

Fig. 2. Expression and purification of Dslo-C280. (*A*) Immunoblot detection of Dslo-C280 band by anti-FLAG M2 antibody in various fractions of *E. coli* before (lane 1) or after (lanes 2–6) induction with IPTG. Lanes: 1, whole cells before IPTG; 2, insoluble protein pellet from lysed cells; 3, soluble protein from lysed cells; 4, whole cells; 5, soluble fraction after high sucrose treatment; and 6, soluble fraction after osmotic shock. (*B*) Purification via FLAG epitope on M2 anti-FLAG affinity column. SDS/PAGE of various fractions. Lanes: 1, molecular mass markers (K = kDa); 2, crude soluble extract; 3, crude inclusion body sample; 4, fraction from soluble extract after M2 column purification; and 5, fraction of renatured inclusion protein after M2 column purification. (*C*) Purification by SEC. SDS/PAGE of fractions from TSK G3000SW column. Lanes: 1, molecular mass markers; 2, SEC peak fraction at ≈68 kDa; and 3, SEC peak fraction at ≈34 kDa. (*D*) Purification via His_6-tag of renatured inclusion protein. SDS/PAGE of various fractions from Ni^{2+}-NTA column. The arrow in *B*, *C*, and *D* points to the Dslo-C280 band.

$^{45}Ca^{2+}$-Binding Activity of Dslo-C280 and a D5N5 Mutant. Many Ca^{2+}-binding proteins can be qualitatively identified by autoradiographic $^{45}Ca^{2+}$-overlay assay performed in a protein blot format (12, 13). This technique is especially useful for identification of proteins containing EF hand Ca^{2+}-binding sites such as calmodulin, troponin C, TCBP-49, and calexcitin (12, 13, 18, 19). It has also been used to identify putative Ca^{2+} binding sites in NH_2- and COOH-terminal domains of Ca^{2+}-ATPase (13, 20) and Ca^{2+}-release channel/ryanodine receptor (21). We find that the DSlo-C280 protein exhibits $^{45}Ca^{2+}$ binding activity in this assay under conditions that selectively label known Ca^{2+}-binding proteins. Fig. 3 compares the $^{45}Ca^{2+}$ signal (*Right*) from two

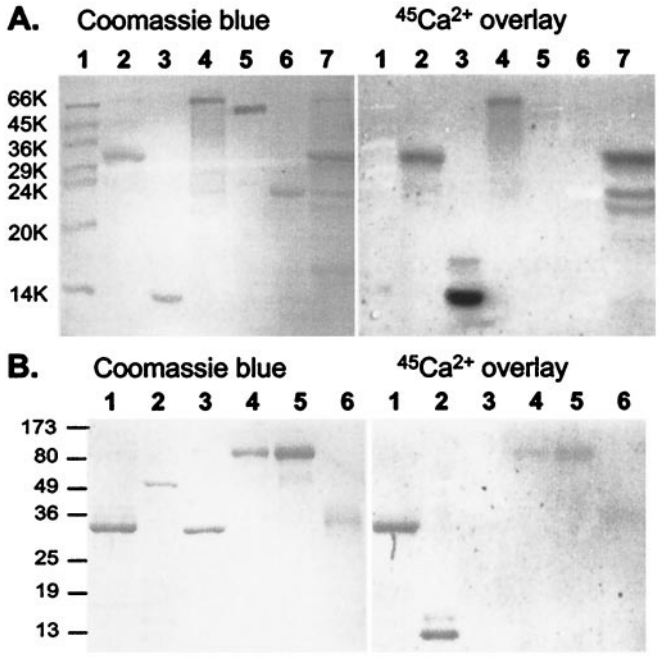

Fig. 3. Protein blot assays demonstrating specificity of $^{45}Ca^{2+}$ binding. Purified Dslo-C280 and various control proteins were subjected to SDS/PAGE, electroblotted onto poly(vinylidene difluoride) membrane, and processed for $^{45}Ca^{2+}$-overlay assay: (*Right*) image of exposed film; (*Left*) same blot stained with Coomassie Blue. (*A*) Lanes: 1, molecular mass markers; 2, Dslo-C280 (≈7 μg); 3, bovine calmodulin (4 μg); 4, rabbit calpain (6 μg); 5, FLAG-tagged *E. coli* alkaline phosphatase (4 μg); 6; bovine trypsin (4 μg); and 7, crude extract from *E. coli* expressing Dslo-C280. (*B*) Lanes: 1, Dslo-C280 (3 μg); 2, chicken troponin complex (6 μg); 3, human annexin V (3 μg); 4, *Aspergillus niger* glucose oxidase (3 μg); 5, glucose oxidase (6 μg); and 6, chicken ovomucoid protease inhibitor (3 μg).

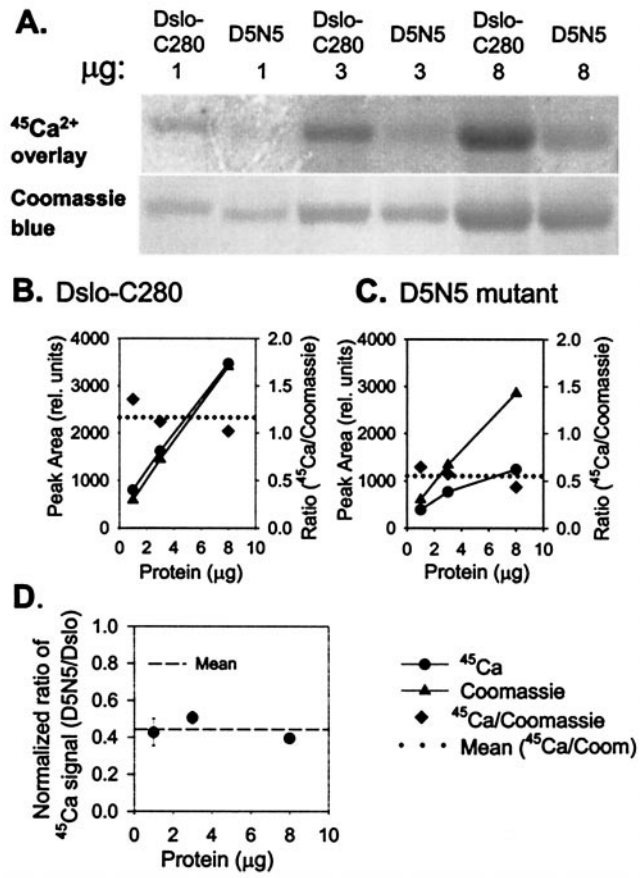

Fig. 4. Comparison of $^{45}Ca^{2+}$-binding activity of Dslo-C280 and corresponding D5N5 mutation. (*A*) Purified Dslo-C280 and D5N5 mutant (1, 3, and 8 μg) were subjected to SDS/PAGE, electroblotted onto PDVF, and assayed by $^{45}Ca^{2+}$-overlay method: (*Upper*) image of exposed film; (*Lower*) Coomassie blue-stained protein bands. (*B* and *C*) Densitometric measurement of protein bands (▲), $^{45}Ca^{2+}$ signal (●), and $^{45}Ca^{2+}$/Coomassie ratio (♦) for Dslo-C280 (*B*) and D5N5 mutant (*C*). (*D*) Protein-normalized ratio of $^{45}Ca^{2+}$-binding activity of D5N5 mutant relative to Dslo-C280.

different protein blots with the same blots stained for protein with Coomassie blue (*Left*). In Fig. 3*A*, it can be seen that both purified Dslo-C280 (lane 2) and a corresponding band from the crude *E. coli* extract (lane 7) retain $^{45}Ca^{2+}$ with a signal comparable to calmodulin (lane 3) and calpain (lane 4). Both calmodulin and the large subunit of calpain, a Ca^{2+}-activated proteinase, contain four EF hand Ca^{2+}-binding motifs. In contrast, other proteins on the same blot, MW markers (lane 1, BSA, chicken ovalbumin, rabbit glyceraldehyde-3-phosphate dehydrogenase, bovine carbonic anhydrase, bovine trypsinogen, soybean trypsin inhibitor, and bovine α-lactalbumin), FLAG-tagged alkaline phosphatase of *E. coli* (lane 5), and bovine trypsin (lane 6) are not labeled by $^{45}Ca^{2+}$ under these conditions. Because Dslo-C280 is an acidic protein with a calculated pI of 4.1, such binding could simply reflect an electrostatic interaction with divalent metal cations rather than specific localized Ca^{2+}-binding sites like those of calmodulin. The experiment of Fig. 3*B* compares the $^{45}Ca^{2+}$ signal of DSlo-C280 (lane 1) with another EF hand protein, troponin C (an ≈18-kDa component of the troponin complex in lane 2), and acidic proteins such as annexin V (pI = 4.8, lane 3), glucose oxidase (pI = 4.2, lanes 4 and 5), and chicken ovomucoid protease inhibitor (pI ≈ 4.3, lane 6). This experiment shows that Dslo-C280 exhibits a stronger $^{45}Ca^{2+}$-binding signal than other acidic proteins tested under the same conditions, further suggesting that the BK channel fragment binds Ca^{2+} in a specific manner.

To investigate the function of the Ca-bowl, we purified a D5N5 mutant of the Dslo-280 fragment in which five consecutive Asp residues of the Ca-bowl region (Fig. 1*C*) were changed to Asn. Schreiber and Salkoff (11) previously found that this same mutation of mouse BK channel (mSlo) reduced the sensitivity to Ca^{2+}-activation by shifting the midpoint of the voltage activation curve ($V_{0.5}$) by an average of +56 mV over the range of 4 to 1,000 μM internal Ca^{2+}. Fig. 4 compares the $^{45}Ca^{2+}$-binding signal of Dslo-C280 and the D5N5 mutant for 1, 3, and 8 μg of protein in a parallel assay on the same blot. The results indicate that the $^{45}Ca^{2+}$ signal is proportional to the amount of both proteins but significantly lower for D5N5 vs. control Dslo-C280. Such data were quantitated by densitometric analysis of the $^{45}Ca^{2+}$ and Coomassie blue protein signals (Fig. 4 *B* and *C*). The results show that the $^{45}Ca^{2+}$-binding signal of the D5N5 mutant was reduced to 44 ± 6% (±SD, n = 3) of control (Fig. 4*D*). Thus, neutralization of five Asp residues of the Ca-bowl to Asn substantially reduces Ca^{2+} binding to a fragment of the Tail domain that is proposed to function as a Ca^{2+} sensor for BK channel activation (11).

Correlation of Ca^{2+}-Binding with Ca^{2+}-Dependent Activation. To determine how the D5N5 mutation affects activation of BK channel opening, we expressed the A1C2E1G3I0 splice version of Dslo and the corresponding D5N5 mutant channel in HEK293 cells and characterized their voltage- and Ca^{2+}-dependence in excised membrane patches. Fig. 5 shows families of macroscopic K^+ currents evoked by a series of depolarizing voltage pulses for the parent Dslo channel with 60 μM internal Ca^{2+} (Fig. 5*A*) and

PHYSIOLOGY

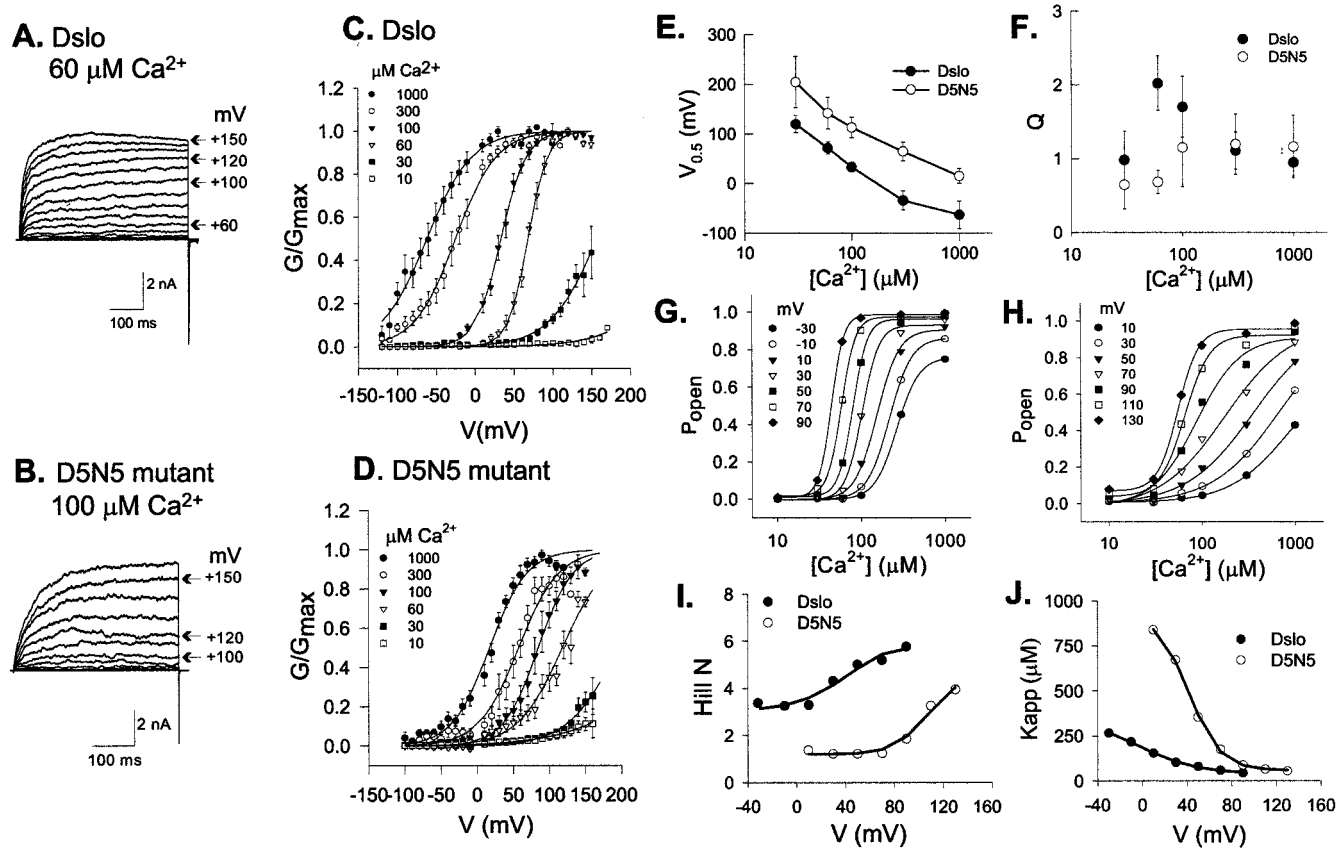

Fig. 5. Analysis of the effect of the D5N5 Ca-bowl mutation on BK channel activation. Dslo and D5N5 mutant BK channels were expressed in HEK293 cells and characterized by patch clamp analysis in inside-out patches. (*A* and *B*) Current traces evoked by consecutive voltage steps of +10 mV from a holding potential of −140 mV for Dslo (*A*) and −120 mV for D5N5 (*B*) with 60 μM and 100 μM Ca^{2+} in the bath solution, respectively. (*C* and *D*) Normalized G-V curves representing the average of 5 to 12 patches at indicated Ca^{2+} concentrations for parent Dslo (C) and D5N5 mutant (*D*). Error bars denote ±SEM. Solid curves are fits to a Boltzmann relationship (Eq. **1**). (*E* and *F*) Comparison of $V_{0.5}$ (*E*) and *Q* (*F*) vs. [Ca^{2+}]. Data points are the mean ±SD of Boltzmann fit parameters from 5–12 patches. (*G* and *H*) Mean values of steady-state P_{open} (G/G_{max}) as a function of [Ca^{2+}] at various voltages compared for Dslo (*G*) and D5N5 mutant (*H*). Solid curves indicate fits to Hill equation (Eq. **2**). (*I* and *J*) Comparison of Hill parameters, *N* (I) and K_{app} (J) vs. voltage.

the D5N5 mutant with 100 μM Ca^{2+} (Fig. 5*B*). At a given Ca^{2+} concentration, the D5N5 mutant requires higher positive voltage than the parent channel to reach maximal activation. This result is shown more directly in Fig. 5 *C* and *D*, which compare averaged voltage activation curves of the two channels at Ca^{2+} concentrations ranging from 10 to 1,000 μM. These data were obtained by normalizing the steady-state conductance (G) at a given voltage to the maximal conductance (G_{max}) measured at high Ca^{2+} for the same patch.

Individual conductance-voltage curves for each patch were fit with the Boltzmann relationship:

$$G/G_{max} = \{1 + \exp[QF(V_{0.5} - V)/RT]\}^{-1}, \qquad [1]$$

where V is applied voltage, $V_{0.5}$ is midpoint voltage, Q is apparent gating charge, F is Faraday's constant, R is the gas constant, and T is absolute temperature. $V_{0.5}$ for activation of the D5N5 channel is shifted by an average of +82 mV relative to the control Dslo channel over the accessible range of Ca^{2+} concentration (Fig. 5*E*). This behavior is similar to that observed by Schreiber and Salkoff (11) for a collection of Ca-bowl mutants of mSlo described as a "(+)-shifted" phenotype. Average values of Q derived from the Boltzmann fit typically fell in the range of 0.9–1.3 and did not show a significant or systematic difference between the mutant and control channel (Fig. 5*F*).

To directly examine the Ca^{2+} dependence of the two types of channels, activation data were also plotted as P_{open} (G/G_{max}) vs. log[Ca^{2+}] over the accessible voltage range and fit to the following modified form of the Hill equation:

$$P_{open} = b + \frac{a[Ca^{2+}]^N}{[Ca^{2+}]^N + K_{app}^N} \qquad [2]$$

In accord with a Monod-Wyman-Changeux (8) theory for Ca^{2+}-activation, Eq. **2** accounts for the fact that, in the limit of zero Ca^{2+}, there is a *minimum* value of P_{open}, described by the b parameter, to which the channel is activated by positive voltage alone (22). Eq. **2** also incorporates a *maximum* value of P_{open}, given by the quantity b + a, that occurs in the limit of high Ca^{2+} and accounts for the observation that the maximum open state probability can still be reduced by negative voltage, even when the Ca^{2+}-binding sites are fully occupied (22). Plots of the [Ca^{2+}] dependence of P_{open} and fits to Eq. **2** are compared in Fig. 5 *G* and *H* for control Dslo and D5N5 mutant channels, respectively. The results show that P_{open} for the D5N5 mutant titrates over a greater and broader range of [Ca^{2+}] than the parent Dslo. This finding can be summarized by comparison of the Hill coefficient, N, and the apparent dissociation constant for Ca^{2+}, K_{app}, as shown in Fig. 5 *I* and *J*, respectively. In Fig. 5*I*, we see that N for the parent Dslo channel ranges from 3.2 to 5.8, whereas N for the D5N5 channel is shifted to lower values ranging from 1.3 to 3.9 over the accessible voltage range. Figure 5*J* shows that K_{app} for

Ca^{2+} increases with negative voltage and is shifted to higher values for the mutant channel.

Discussion

This work demonstrates that a COOH-terminal portion of the *Drosophila* BK channel binds $^{45}Ca^{2+}$ in a protein blot assay. Under defined conditions (ionic strength, pH, Mg^{2+} concentration, and washing), this assay reliably identifies many different Ca^{2+}-binding proteins, particularly those with EF-hand motifs (12, 13). The fact that Dslo-C280 exhibits a strong $^{45}Ca^{2+}$-binding signal relative to control proteins (Fig. 3) supports the idea that this part of the Dslo Tail domain contains Ca^{2+}-binding site(s) discretely localized within its linear sequence. The molecular basis of Ca^{2+} binding to calmodulin and other EF-hand proteins in the protein blot format is unknown; however, it has been suggested that discretely localized Ca^{2+}-binding sites can partially refold and reconstitute Ca^{2+}-coordination within the blotted protein band in the same way that denaturation-resistant epitopes are recognized by certain antibodies after transfer of antigen proteins from SDS/PAGE gels (12).

Although the BK channel protein does not contain a canonical EF-hand motif (4), a conserved region of sequence rich in Asp residues in the Tail domain, known as the Ca-bowl, has emerged as a candidate Ca^{2+}-binding site (10, 11). Based on studies of the interaction of BK channels with certain serine protease inhibitors, Moss *et al.* (23) previously suggested that the Ca-bowl region may be structurally related to the relatively low affinity ($K_D \approx 100\ \mu M$) Ca^{2+}-binding loop of serine proteinases such as trypsin, coagulation Factors VII, IX, X, and protein C (24). Such proposals for a Ca^{2+}-binding function of the Ca-bowl are supported by results of Fig. 4, which show that mutation of five consecutive Asp residues in this region to Asn result in a 56% reduction in $^{45}Ca^{2+}$-signal in the overlay assay.

Structure-function analyses of the Ca-bowl region of the mammalian BK channel (mSlo) have been interpreted to suggest that the Tail domain contains at least two distinct Ca^{2+}-binding sites (10, 11). In addition to showing that the Ca-bowl region is functionally important for Ca^{2+}-binding and Ca^{2+}-dependent activation of an insect BK channel, the present work supports the idea that there is more than one Ca^{2+}-binding site per Tail domain. This possibility is suggested by the fact that the D5N5 mutation does not completely eliminate $^{45}Ca^{2+}$-binding (Fig. 4) and by the particular effect of this mutation on the Hill coefficient for Ca^{2+} activation. As shown in Fig. 5 *G* and *I*, the Hill coefficient of the control Dslo channel increases as a function of positive voltage, increasing from $N \approx 3$ at -40 mV to $N \approx 6$ at $+80$ mV. A systematic increase in the Hill coefficient of activation by Ca^{2+} (and Sr^{2+}) over a similar voltage range has been previously observed in other studies of BK channels from diverse species (22, 25–28). This behavior can be simulated by a Monod-Wyman-Changeux type of model of Ca^{2+} activation and arises from the allosteric coupling of Ca^{2+}- and voltage-dependent activation (S.B. and E.M., unpublished results). Here, we observed that Hill coefficient values of the D5N5 channel are sharply reduced from the parent Dslo channel (Fig. 5*I*). One way to account for the results of Fig. 5 is by postulating that the Dslo BK channel contains at least two distinct Ca^{2+}-binding sites per Tail domain, for a minimum of eight sites per tetramer. This relationship gives a molecularity of 8 to the Ca^{2+}-activation process and leads to the theoretical possibility of Hill coefficients ≥ 4 observed here and in many previous studies of BK channels (29–32). If the D5N5 mutation essentially eliminates one of two Ca^{2+}-binding sites in the Tail domain, this mutation would result in a channel in which the allowable range of the Hill coefficient is reduced to less than 4, as observed in Fig. 5*I*.

In conclusion, this set of experiments provides a direct correlation between a biochemical measurement of Ca^{2+} binding to the Tail domain and Ca^{2+}-dependent activation of a BK channel. The results support the idea (but do not yet prove) that the Ca-bowl sequence motif directly participates in Ca^{2+} binding and that BK channels contain at least two Ca^{2+}-binding sites per monomer of a homotetrameric complex. Further quantitative biochemical and structural studies of the Tail domain produced in *E. coli* ought to reveal more details relevant to the mechanism of BK channel gating.

We thank Dr. Chien-Jung Huang for assistance with electrophysiology experiments. This work was supported by a grant from the National Institutes of Health (GM51172) and by fellowship awards from the American Heart Association to S.B. and I.F.

1. Toro, L., Wallner, M., Meera, P. & Tanaka, Y. (1998) *News Physiol. Sci.* **13,** 112–117.
2. Meera, P., Wallner, M., Jiang, Z. & Toro, L. (1996) *FEBS Lett.* **382,** 84–88.
3. Cui, J., Cox, D. H. & Aldrich, R. W. (1997) *J. Gen. Physiol.* **109,** 647–673.
4. Butler, A., Tsunoda, S., McCobb, D. P., Wei, A. & Salkoff, L. (1993) *Science* **261,** 221–224.
5. Meera, P., Wallner, M., Song, M. & Toro, L. (1997) *Proc. Natl. Acad. Sci. USA* **94,** 14066–14071.
6. Horrigan, F. T., Cui, J. & Aldrich, R. W. (1999) *J. Gen. Physiol.* **114,** 277–304.
7. Rothberg, B. S. & Magleby, K. L. (1999) *J. Gen. Physiol.* **114,** 93–124.
8. Monod, J., Wyman, J. & Changeux, J. P. (1965) *J. Mol. Biol.* **12,** 88–118.
9. Wei, A., Solaro, C., Lingle, C. & Salkoff, L. (1994) *Neuron* **13,** 671–681.
10. Schreiber, M., Yuan, A. & Salkoff, L. (1999) *Nat. Neurosci.* **2,** 416–421.
11. Schreiber, M. & Salkoff, L. (1997) *Biophys. J.* **73,** 1355–1363.
12. Maruyama, K., Mikawa, T. & Ebashi, S. (1984) *J. Biochem.* **95,** 511–519.
13. Garrigos, M. S., Deschamps, S., Veil, A., Lund, S., Champeil, P., Moller, J. V. & le Maire, M. (1991) *Anal. Biochem.* **194,** 82–88.
14. Adelman, J. P., Shen, K.-Z., Kavanaugh, M. P., Warren, R. A., Wu, Y.-N., Lagrutta, A., Bond, C. T. & North, R. A. (1991) *Neuron* **9,** 209–216.
15. Nelson, R. M. & Long, G. L. (1989) *Anal. Biochem.* **180,** 147–151.
16. Moss, G. W. J., Marshall, J., Morabito, M., Howe, J. R. & Moczydlowski, E. (1996) *Biochemistry* **35,** 16024–16035.
17. Colangeli, R., Heijbel, A., Williams, A. M., Manca, C., Chan, J., Lyashchenko, K. & Gennaro, M. L. (1998) *J. Chromatogr. B* **714,** 223–235.
18. Dodds, D., Schlimgen, A. K., Lu, S.-Y. & Perin, M. S. (1995) *J. Neurochem.* **64,** 2339–2344.
19. Nelson, T. J., Cavallaro, S., Yi, C.-L., McPhie, D., Schreuers, B. G., Gusev, P. A., Favit, A., Zohar, O., Kim, J., Beushausen, S., Ascoli G., Old, J., Neve, R. & Alkon, D. L. (1996) *Proc. Natl. Acad. Sci. USA* **93,** 13808–13813.
20. Hofmann, F., James, P., Vorherr, T. & Carafoli, E. (1993) *J. Biol. Chem.* **268,** 10252–10259.
21. Chen, S. R. & MacLennan, D. H. (1994) *J. Biol. Chem.* **36,** 22698–22704.
22. Cox, D. H., Cui, J. & Aldrich, R. W. (1997) *J. Gen. Physiol.* **110,** 257–281.
23. Moss, G. W. J., Marshall, J. & Moczydlowski, E. (1996) *J. Gen. Physiol.* **108,** 473–484.
24. Persson, E., Hogg, P. J. & Stenflo, J. (1993) *J. Biol. Chem.* **268,** 22531–22539.
25. Moczydlowski, E. & Latorre, R. (1983) *J. Gen. Physiol.* **82,** 511–542.
26. Sugihara, I. (1994) *J. Physiol. (London)* **476,** 373–390.
27. Sugihara, I. (1998) *J. Gen. Physiol.* **111,** 363–379.
28. Cui, J., Cox, D. H. & Aldrich, R. W. (1997) *J. Gen. Physiol.* **109,** 647–673.
29. McManus, O. B. & Magleby, K. L. (1991) *J. Physiol. (London)* **443,** 739–777.
30. Carl, A. & Sanders, K. M. (1989) *Am. J. Physiol.* **257,** C470–C480.
31. Wu, J. V., Shuttleworth, T. J. & Stampe, P. (1996) *J. Membr. Biol.* **154,** 275–282.
32. Golowasch, J., Kirkwood, A. & Miller, C. (1986) *J. Exp. Biol.* **124,** 5–13.